

Article

Not peer-reviewed version

A Generalizable Efficient Machine Learning Framework for Schizophrenia Classification Using Multiscale EEG Features and Ensemble Methods

Yossef Emara [†], Xinran Han [†], Alice Zhang, [Yi Lin](#), [Yang Zhang](#) ^{*}

Posted Date: 6 February 2026

doi: 10.20944/preprints202602.0513.v1

Keywords: schizophrenia; electroencephalography (EEG); ensemble learning



Preprints.org is a free multidisciplinary platform providing preprint service that is dedicated to making early versions of research outputs permanently available and citable. Preprints posted at Preprints.org appear in Web of Science, Crossref, Google Scholar, Scilit, Europe PMC.

Copyright: This open access article is published under a [Creative Commons CC BY 4.0 license](#), which permit the free download, distribution, and reuse, provided that the author and preprint are cited in any reuse.

Disclaimer/Publisher's Note: The statements, opinions, and data contained in all publications are solely those of the individual author(s) and contributor(s) and not of MDPI and/or the editor(s). MDPI and/or the editor(s) disclaim responsibility for any injury to people or property resulting from any ideas, methods, instructions, or products referred to in the content.

Article

A Generalizable Efficient Machine Learning Framework for Schizophrenia Classification Using Multiscale EEG Features and Ensemble Methods

Yossef Emara ^{1,†}, Xinran Han ^{2,†}, Alice Zhang ³, Yi Lin ⁴ and Yang Zhang ^{2,*}

¹ Department of Computer Science and Engineering, University of Minnesota, Minneapolis, MN 55455, USA

² Department of Speech-Language-Hearing Sciences and Masonic Institute for the Developing Brain, University of Minnesota, Minneapolis, MN 55455, USA

³ Wayzata High School, 4955 Peony Ln N, Plymouth, MN 55446, USA

⁴ Speech-Language-Hearing Center, School of Foreign Languages, Shanghai Jiao Tong University, Shanghai, People's Republic of China; National Research Centre for Language and Well-Being, Shanghai, People's Republic of China

* Correspondence: zhanglab@umn.edu

† These authors contributed equally to this work.

Abstract

EEG-based automated classification pipelines for identifying mental disorders increasingly rely on deep learning architectures that are computationally intensive and difficult to interpret, limiting reproducibility and clinical deployment in resource-constrained or cross-site settings. There is a need for algorithmically transparent frameworks that balance accuracy, generalization, and computational efficiency. We propose an interpretable EEG classification framework that integrates multiscale spectrotemporal feature extraction with ensemble machine learning. The pipeline combines standardized preprocessing with extraction of time-domain, spectral power, and entropy-based features, followed by minimum redundancy–maximum relevance feature selection. Classification is performed using voting and stacking ensembles of heterogeneous base learners. The proposed algorithm achieved 98.06% accuracy on a primary open EEG dataset (Warsaw IPN; 19 channels, 250 Hz) and 91.47% accuracy on an independent external dataset (Moscow adolescent cohort; 16 channels, 128 Hz) without retraining or dataset-specific tuning. The framework exhibited low computational overhead and stable cross-dataset performance. The results demonstrate a generalizable, computationally efficient, and interpretable EEG classification framework that favors feature-level transparency and ensemble diversity over deep architectures, supporting scalable and reproducible biomedical signal processing applications.

Keywords: schizophrenia; electroencephalography (EEG); ensemble learning

1. Introduction

Schizophrenia (SZ or SCZ) is a severe and heterogeneous neuropsychiatric disorder affecting approximately 0.3–0.7% of the global population [1]. It is characterized by positive symptoms (e.g., hallucinations and delusions), negative symptoms (e.g., avolition and blunted affect), and persistent cognitive impairments that disrupt daily functioning. Beyond core psychotic symptoms, individuals with SZ exhibit robust deficits in language and social recognition [2], including impaired recognition of facial and vocal emotions [3–7]. Although the behavioral markers are clinically informative, their subjective nature introduces inter-rater variability, limits sensitivity to early and subclinical disease stages, and lacks mechanistic grounding in neural processes. This motivates the need for objective, biologically grounded measures to support scalable diagnosis and monitoring.

Electroencephalography (EEG) has emerged as a promising modality due to its millisecond temporal resolution, non-invasiveness, portability, and sensitivity to neural oscillatory dynamics [8,9]. EEG captures abnormalities in brain rhythms, functional connectivity, and signal complexity that are consistently reported in SZ (e.g., [10–13]) and reflect dysregulation of large-scale neural networks. However, the high dimensionality, multiscale structure, and noise characteristics of EEG limit the effectiveness of conventional statistical approaches. Machine learning (ML) methods are therefore well-suited to learn latent patterns that distinguish schizophrenia-related neural dysfunction. Recent years have seen rapid growth in EEG-based ML for automated SZ detection, mechanistic interpretation, and clinical outcome prediction (see [14] for a systematic review).

1.1. Methodological Frameworks in EEG-Based SZ Classification

Most EEG-based SZ classification studies follow a three-stage pipeline: preprocessing, feature extraction, and classification [15–18]. Preprocessing is essential for reducing contamination from ocular, muscular, and environmental artifacts. Standard procedures include band-pass filtering (commonly 0.5–50 Hz or 1–40 Hz) [17,19,20], re-referencing (e.g., average reference), artifact correction or rejection using Independent Component Analysis (ICA) or related algorithms, and segmentation into epochs for resting-state or event-related analysis [17,18]. Signal normalization (e.g., z-scoring) is often applied to mitigate inter-subject variability (e.g., [21]), although preprocessing choices remain a major source of between-study inconsistency.

EEG abnormalities in SZ manifest across multiple temporal and spatial scales, necessitating complementary feature representations. Feature extraction aims to capture the multiscale neural abnormalities associated with SZ and typically spans several complementary domains: (1) Time-domain features, including statistical descriptors and event-related potentials (ERPs) [22] such as reduced P300 and N100 amplitudes and delayed latencies, reflecting impairments in attention and sensory processing [23,24]. (2) Frequency-domain features, such as power spectral density (PSD) across canonical frequency bands [25], with reduced resting-state alpha power and elevated theta activity, particularly in frontal regions [9,26,27]. (3) Time–frequency features, derived from wavelet or short-time Fourier transforms, capturing transient, non-stationary dynamics that are not visible in static spectral measures [28,29]. (4) Functional connectivity and network features, such as coherence, phase-locking value (PLV), and graph-theoretic metrics, showing widespread dysconnectivity, especially within fronto-temporal and fronto-parietal networks, supporting the dysconnection hypothesis of SZ [30–32]. (5) Nonlinear and complexity features, including entropy measures, fractal dimension, and detrended fluctuation analysis (DFA), consistently indicating reduced neural complexity and diminished adaptive flexibility in SZ [33,34]. (6) Emerging representations, such as EEG microstates, model quasi-stable scalp topographies, showing altered temporal dynamics in SZ, particularly in microstates associated with salience and cognitive control networks [35–37].

Classification models range from traditional supervised ML to deep learning (DL) and hybrid or ensemble approaches. Traditional classifiers such as Support Vector Machines (SVM) [31,36,38–42], Random Forests (RF) [43–45], k-Nearest Neighbors (k-NN or KNN) [46], and Logistic Regression are widely used due to their interpretability, computational efficiency, and suitability for small datasets. These models rely on handcrafted features and often incorporate feature selection methods to reduce dimensionality (e.g., [39,47–49]). In contrast, DL architectures, including Convolutional Neural Networks (CNNs) [50–52] and Recurrent Neural Networks (RNNs), automatically learn hierarchical spatiotemporal representations directly from raw or minimally processed EEG. For example, hybrid CNN-LSTM (Long Short-Term Memory) architectures have shown state-of-the-art performance in tasks like classification and anomaly detection [53–56]. While DL models have achieved state-of-the-art performance, they require large labeled datasets, substantial computational resources, and often lack interpretability, posing barriers to clinical adoption [14,57]. Hybrid and ensemble methods attempt to balance these trade-offs by combining complementary feature sets or classifiers and employing techniques such as voting, bagging, or stacking to improve robustness [14,58].

1.2. Key Limitations in Existing EEG–ML Studies

A primary source of heterogeneity across EEG-based schizophrenia (SZ) classification studies lies in feature learning strategies (Table 1). Traditional machine learning approaches rely on hand-crafted, domain-informed features, including spectral representations (e.g., FFT-based features), signal decomposition methods (e.g., ICA, RVMD, wavelet transforms), and statistical or texture-based descriptors such as Statistical Local Binary Patterns (SLBP) [17,59–63]. These features are typically classified using conventional algorithms such as SVM, KNN, Linear Discriminant Analysis (LDA), decision trees, and ensemble methods, which remain prevalent across both public (e.g., IPN, Kaggle SCZ) and private datasets [62,64,65]. In contrast, deep learning (DL) models, including Deep ResNets, GoogleNet, and RNN-LSTM architectures, aim to learn hierarchical feature representations directly from minimally processed EEG signals (e.g., [54,66–69]). Hybrid approaches that combine deep feature extraction with classical classifiers have also been explored to balance representational capacity with limited dataset sizes [66,67]. However, the reported performance gains of DL-based models are often closely tied to data availability and computational resources rather than intrinsic methodological advantages [70].

Substantial variability also arises from differences in EEG preprocessing pipelines. Common practices include bandpass filtering (e.g., Butterworth and FIR filters), artifact removal via ICA, and more advanced decomposition techniques such as RVMD and flexible tunable Q wavelet transform (F-TQWT) [60,61,71–73]. These preprocessing choices directly influence feature distributions and learned decision boundaries [74], making reported performance difficult to disentangle from signal conditioning methods and complicating cross-study comparison.

Experimental paradigms further contribute to inconsistency. Task-based EEG paradigms (e.g., auditory oddball or working memory tasks) target specific cognitive processes and event-related potentials such as P300 and N100 [12,75–79], offering mechanistic interpretability but requiring task compliance. Resting-state EEG, which dominates many studies in Table 1, captures intrinsic brain dynamics without task demands [80], improving clinical feasibility but increasing inter-subject variability. These paradigm differences substantially affect both feature representations and neurobiological interpretations.

Validation protocols represent another major limitation. Most studies rely on k-fold cross-validation to estimate internal robustness (e.g., [60,68]), whereas more stringent approaches such as leave-one-subject-out (LOSO) or leave-one-out (LOO) validation are less frequently adopted. All within-dataset validation strategies are susceptible to optimistic bias, particularly in small, high-dimensional EEG datasets. External validation on independent cohorts remains rare [14], limiting confidence in cross-site generalizability and real-world applicability.

Despite these methodological differences, many EEG–ML studies report high classification performance, often exceeding 80–90% accuracy (Table 1). Rather than indicating a universally superior approach, these results reflect convergent neurophysiological findings in SZ, including reduced alpha-band power, increased theta activity, disrupted fronto-temporal and fronto-parietal connectivity, and decreased signal complexity [8,9,12]. These abnormalities are consistently exploited across diverse modeling frameworks, either explicitly through hand-crafted features or implicitly through learned representations. Emerging work also suggests that EEG-based ML may extend beyond binary classification to cognitive profiling, subtype identification, and symptom prediction [70].

Table 1. Summary of schizophrenia classification studies with EEG signals.

Study	Accuracy (%)	Preprocessing Method	Model Used	Database
[59]	99.25	Fast Fourier transform (FFT) and statistical feature	SVM, KNN, Boosted Tree (BT), and Decision Tree (DT)	IPN and Kaggle SCZ dataset
[66]	99.23	Average filtering	Deep ResNets, softmax layer and deep features with SVM	Kaggle SCZ dataset
[67]	98.84	Average filtering	GoogleNet and deep features, SVM	Kaggle SCZ dataset
[61]	89.21	EEGLAB and ICA	KNN, LDA, and SVM	Private

[60]	92.93	Robust variational mode decomposition (RVMD)	Optimized extreme machine classifier	Kaggle SCZ dataset
[82]	90.93	Bandpass filter	SVM and Bayesian optimization	IPN
[68]	98	Dimensionality reduction algorithm	RNN-LSTM	LNNCI [83]
[48]	92.17	ICA	Black Hole (BH) optimization and SVM	IPN
[84]	91.66	Symmetrically Weighted local binary patterns (SLBP) and correlation	Logit Boost classifier	LNNCI, MHRC
[85]	93.9	Finite impulse response (FIR) filter	KNN, Artificial Neural Network (ANN), and SVM	Kaggle SCZ dataset
[65]	99.91	CGP17Pat and Iterative neighborhood component analysis (INCA)	KNN	IPN
[39]	92.91	Butterworth filter and Segmentation	DT, Linear-Discriminant Analysis (LDA), KNN, Probabilistic-Neural-Network (PNN), and SVM	
[86]	71	Butterworth filter and Independent component analysis (ICA)	LDA, and Rule-based classifier	Private
[87]	72.4	Digital filters and ICA	KNN, LDA, SVM	Private
[88]	93.4	Spatial filters and Bandpass filter	SVM, Bayesian LDA, Gaussian NB, KNN, Adaboost, and Radial basis function (RBF)	Private
[89]	91.39	Flexible tunable Q wavelet transform (F-TQWT)	Flexible least square support vector machine (F-LSSVM) classifier and grey wolf optimization (GWO) algorithm	Kaggle SCZ dataset

However, significant barriers continue to limit clinical translation. Most studies rely on small, single-site datasets, often private cohorts, reducing robustness and population-level generalizability. Inter-subject variability related to age, medication status, illness duration, and symptom severity further complicates model learning. Combined with high-dimensional feature spaces, limited sample sizes increase the risk of overfitting and inflated performance estimates that fail to replicate across datasets. Furthermore, the lack of standardization in preprocessing, feature extraction, validation protocols, and evaluation metrics undermines reproducibility. Model interpretability remains a critical concern: while DL-based methods capture complex patterns, their black-box nature limits neurobiological insight and clinician trust. Moreover, the predominant focus on binary classification reduces ecological validity, as clinical diagnosis requires discrimination among multiple psychiatric conditions.

Taken together, although EEG-based machine learning approaches show strong potential for SZ classification, their performance remains highly sensitive to methodological choices and dataset characteristics. Ensemble learning offers a principled strategy to mitigate these limitations by integrating multiple classifiers or complementary feature views, thereby reducing bias and variance and improving robustness in small-to-moderate sample size regimes typical of EEG studies. Despite these advantages, ensemble methods remain underexplored in EEG-based schizophrenia classification (e.g., [59,81]). Advancing toward clinical deployment will therefore require standardized pipelines, rigorous external validation, systematic evaluation of ensemble frameworks, improved interpretability, and clinically realistic multi-class diagnostic settings.

1.3. The Present Study

Motivated by persistent challenges in EEG-based schizophrenia classification—particularly limited cross-dataset generalizability and the practical constraints of data-intensive deep learning models—we propose a generalizable and interpretable machine learning framework for schizophrenia detection from EEG. The framework emphasizes robust multiscale feature extraction from resting-state EEG, integrating time-domain, spectral, connectivity, entropy-based, and fractal measures, including detrended fluctuation analysis (DFA). To improve robustness while preserving

interpretability and computational efficiency, ensemble learning is employed within a feature-based machine learning paradigm.

Crucially, the proposed framework is evaluated using a stringent cross-dataset validation strategy: models are trained and optimized on one open-source EEG dataset and tested without retraining or parameter tuning on an independent cohort. This evaluation protocol prioritizes generalization over inflated within-dataset performance and provides a realistic assessment of clinical applicability. By delivering a reproducible, plug-and-play pipeline compatible with standard EEG recordings, this work aims to advance EEG-based computational psychiatry from proof-of-concept demonstrations toward scalable and objective tools for schizophrenia detection and neurophysiological analysis.

The remainder of the paper is organized as follows. Section 2 describes the datasets, preprocessing procedures, multidomain feature extraction, feature selection, and classification models, including baseline and ensemble approaches, along with the evaluation protocol. Section 3 presents performance results on both the primary and independent validation datasets, reporting accuracy, F1-score, and ROC–AUC metrics. Section 4 discusses the methodological advantages, clinical implications, and limitations of the proposed framework, and Section 5 concludes the paper.

2. Materials and Methods

2.1. EEG Data-Sets and Preprocessing

The primary dataset used in this study was obtained from the public repository of Olejarczyk and Jernajczyk at the Institute of Psychiatry and Neurology in Warsaw [32,80]. This dataset consists of resting-state EEG recordings from 14 healthy controls and 14 patients diagnosed with paranoid schizophrenia (ICD-10: F20.0), with an average recording duration of 1028.7 seconds per subject. Signals were sampled at 250 Hz from 19 scalp channels: Fp2, F8, T4, T6, O2, Fp1, F7, T3, T5, O1, F4, C4, P4, F3, C3, P3, Fz, Cz, and Pz. The data were stored in EDF format and loaded using the MNE Python library (originally based on the Minimum Norm Estimate method for MEG/EEG analysis) [90]. For preprocessing, the EEG recordings were segmented into 6-second epochs with 2-second overlap, resulting in 7191 epochs, each containing 19 channels with 1500 time points. A bandpass filter (0.5–50 Hz) was applied to remove slow drifts and high-frequency noise, followed by artifact removal using Independent Component Analysis (ICA) via MNE and the Automatic and Tunable Artifact Removal (ATAR) algorithm from the SpKit Python library.

To evaluate the generalizability of the proposed framework, an independent validation dataset was also used. This dataset was obtained from Moscow University (http://brain.bio.msu.ru/eeg_schizophrenia.htm) and includes resting-state EEG recordings from adolescents, clinically screened and categorized as healthy controls ($n = 39$) or adolescents exhibiting schizophrenia symptoms ($n = 45$). EEG signals were acquired with 16 scalp electrodes (F7, F3, F4, F8, T3, C3, Cz, C4, T4, T5, P3, Pz, P4, T6, O1, O2) at a sampling rate of 128 Hz, with each recording lasting approximately one minute per subject (7680 samples per channel). The raw EEG data were stored as text files with sequentially concatenated channels. All preprocessing steps, feature extraction procedures, and classification models developed for the primary dataset were directly applied to this independent dataset to assess the robustness and cross-dataset generalization of the proposed approach.

2.1.1. ICA and ATAR

Independent Component Analysis ICA is a Blind Source Separation (BSS) method used in signal processing and artifact removal [91] and has been used extensively in the literature surrounding EEG machine learning classification due to its availability in several well established software libraries (e.g., EEGLAB [92], FieldTrip [93], and MNE-Python [94]). This algorithm decomposes EEG signals with multiple channels into independent source signals which can be visually excluded through scalp topography, with newer techniques [95] able to automatically do so when manual selection is

unrealistic in large datasets. Despite its popularity, ICA can sometimes be overly aggressive, introducing spurious frequency components or distorting neural signals, which may negatively impact downstream predictive models [96].

A more novel approach that is seldom used is ATAR (Automatic and Tunable Artifact Removal Algorithm) (Figure 1), which uses Wavelet Packet Decomposition to capture temporal patterns in EEG signals [97]. Unlike ICA, ATAR provides a tunable parameter (β) that allows the user to control the aggressiveness of artifact removal, balancing the elimination of ocular and muscle artifacts with the preservation of essential neural signals. In our experiments, ATAR outperformed ICA in improving machine learning model performance, likely due to the controlled artifact removal enabled by setting $\beta = 0.1$, which preserved critical EEG features while efficiently mitigating noise. Our experiments revealed that ATAR provided better results in the machine learning process compared to ICA in efficiently removing ocular and muscle artifacts.. This is likely due to the tunability of the (β) parameter (which was set to 0.1), which enabled a more balanced approach to artifact removal and signal preservation.

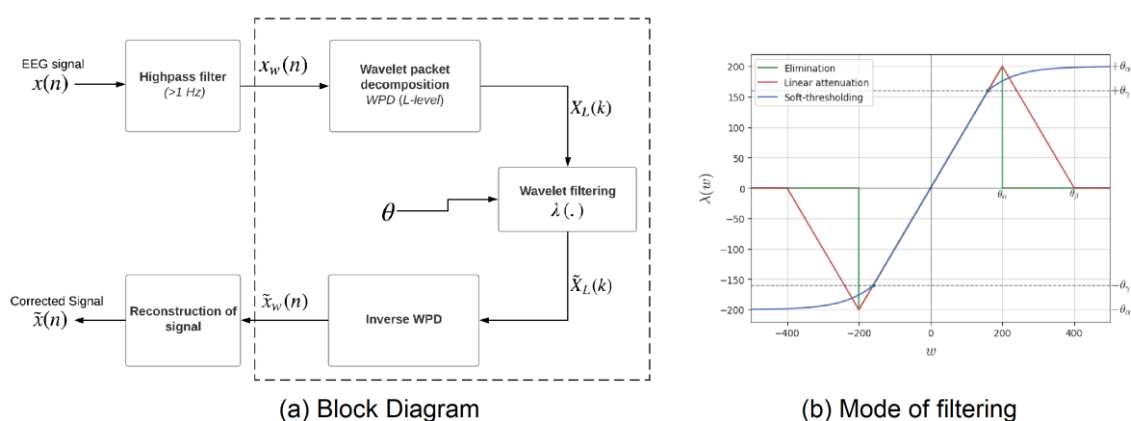


Figure 1. ATAR Algorithm Block Diagram.

2.2. Feature Extraction

To effectively capture the complex and high-dimensional nature of EEG signals, features were extracted from the time domain, frequency domain, and entropy measures, providing a comprehensive representation of neural dynamics [98,99]. Time-domain features included standard statistical metrics such as sum of absolute differences, mean, variance, standard deviation, minimum and maximum signal values, root mean square (RMS), as well as Hjorth parameters—activity (HA), mobility (HM), and complexity (HC)—which characterize signal amplitude, spectral content, and waveform irregularity [100]. Additionally, higher-order statistics such as skewness and kurtosis were computed to capture asymmetry and peakedness of the signal distribution. Entropy features, including Shannon entropy, Wavelet entropy, and Fuzzy entropy, were extracted to quantify the unpredictability and complexity of EEG time series, which have been shown to reflect underlying neurological states [101]. Frequency-domain features were derived from the power spectral density (PSD) and included band powers within the delta (δ , 0.5–4 Hz), theta (θ , 4–8 Hz), alpha (α , 8–13 Hz), and beta (β , 13–30 Hz) bands, as well as additional statistical measures and spectral entropy to capture the distribution and complexity of spectral content [102]. Together, these multidomain features provide a rich representation for machine learning models to distinguish between healthy and pathological EEG patterns.

2.2.1. Time Domain Features

Statistical feature extraction from the time domain of the signal have proven to yield promising results when used as features in the task of EEG machine learning classification [103]. The following features were extracted from the signal from every channel:

(a) Sum of Absolute Differences (SAD):

$$SAD = \sum_{i=1}^n |x_i - y_i| \quad (1)$$

where n represents the total number of data points in the time series, x_i is the value of the signal at the i -th time point, and y_i is the corresponding value of a reference signal or the signal at a previous time point. This feature quantifies the variability and rapid changes in the brain's electrical activity expressed in time series data.

(b) Root Mean Square (RMS):

RMS captures the overall amplitude and energy contained within a signal, which is correlated with the intensity of neural activity.

$$RMS(x) = \sqrt{\frac{1}{n} \sum_{i=1}^n x_i^2} \quad (2)$$

(c) Hjorth Parameters (Activity, Mobility, and Complexity):

Hjorth parameters are used almost exclusively and developed specifically for characterizing EEG signals and can give us a glimpse of the spectral qualities of a signal without needing computationally expensive methods like Fast Fourier Transform.

Hjorth Activity is able to describe the power of an EEG signal through the variance of the time function.

$$Activity = \sigma^2 = \frac{1}{N} \sum_{i=1}^N (x_i - \bar{x})^2 \quad (3)$$

where x_i are the signal values, \bar{x} is the mean of the signal, and N is the number of samples.

Hjorth Mobility describes the movement and variation of the spectral components of a signal, and describes the mean frequency of the signal as well the proportion of the standard deviation of the power spectrum.

$$Mobility = \sqrt{\frac{\sigma_{\dot{x}}^2}{\sigma^2}} \quad (4)$$

where \dot{x} is the first derivative of the signal with respect to time, i.e., $\dot{x}(t) = \frac{dx(t)}{dt}$, $\sigma_{\dot{x}}^2$ is the variance of the derivative signal $\dot{x}(t)$, and σ^2 is the variance of the original signal $x(t)$.

Hjorth Complexity computes the similarity between an EEG signal and a pure sine wave which is a measure of complexity and irregularity.

$$Complexity = \frac{\sqrt{\frac{1}{N} \sum_{i=1}^N (\ddot{x}_i - \bar{\ddot{x}})^2}}{\sqrt{\sigma_{\dot{x}}^2}} \quad (5)$$

where \ddot{x}_i are the values of the second derivative of the signal, $\bar{\ddot{x}}$ is the mean of the second derivative, and N is the number of samples.

2.2.2. Frequency Domain Features

Frequency-domain feature extraction plays a crucial role in EEG signal analysis, as it provides insight into how signal power is distributed across different frequency bands, which can be associated with specific cognitive states or neurological conditions [97]. To characterize these frequency-domain properties, the power spectral density (PSD) of each EEG channel was computed

using Welch's method. This approach estimates the PSD by dividing the signal into overlapping segments, applying a window function to each segment, performing a Fast Fourier Transform (FFT) on each window, and averaging the resulting spectra across all segments. Welch's method is particularly well suited for EEG analysis because it reduces variance in the spectral estimate and is effective for handling the non-stationary nature of EEG signals.

Formally, given a signal $x[n]$ of length N , the signal is divided into K overlapping segments, each of length M . For each segment, a periodogram is computed as

$$P_k(\omega) = \frac{1}{M} \left| \sum_{n=(k-1)M+1}^{kM} x[n] e^{-j2\pi n k / N} \right|^2 \quad (6)$$

where $k = 1, 2, \dots, K$. N represents the total length of the signal, K denotes the number of segments, M is the length of each segment, and ω corresponds to the frequency variable.

The final PSD estimate is then obtained by averaging the individual periodograms across all segments:

$$P(\omega) = \frac{1}{K} \sum_{k=1}^K P_k(\omega) \quad (7)$$

Once the PSD was estimated, band power features were computed by calculating the area under the PSD curve within specific frequency ranges. In particular, power values were extracted for the Delta (δ), Theta (θ), Alpha (α), and Beta (β) frequency bands. In addition to band powers, spectral entropy and other statistical measures were derived from the PSD of each EEG channel to capture the complexity and distribution of spectral content. Finally, additional statistical features listed in Table 1, including the mean, skewness, and kurtosis of the frequency-domain representation, were also extracted to further characterize the spectral properties of the EEG signals.

2.2.3. Entropy Features

Entropy in EEG signals measures the complexity and unpredictability of the brain's electrical activity. These entropic measures have been successfully used in the classification of Parkinson's Disorder as well as human emotion due to their ability to capture complex characteristics in the signals that are symptomatic of neurological states [104]. For feature extraction we extracted Shannon, Wavelet, Permutation, and Fuzzy Entropy from every channel.

2.3. Feature Selection

To reduce the high dimensionality of the feature space and mitigate overfitting in machine learning models, multiple feature selection strategies were systematically evaluated [105]. Initially, low-variance filtering was applied to remove features with minimal variability across samples, as these features are unlikely to contribute meaningful discriminative information. Next, univariate feature selection using mutual information (MI) was employed, quantifying the dependency between each feature X and the class label Y as:

$$I(X; Y) = \sum_{y \in Y} \sum_{x \in X} p(x, y) \log \left(\frac{p(x, y)}{p(x)p(y)} \right), \quad (8)$$

where X denotes the feature and Y the class label and x, y represents specific values that the variables X and Y can take.

Mutual information effectively identifies features that provide the most information about class distinctions, capturing both linear and nonlinear relationships [106].

Following MI-based selection, Recursive Feature Elimination (RFE) was applied using tree-based models to iteratively remove the least informative features, retaining only those that contribute most to model performance [107]. RFE leverages the inherent feature importance scores of tree ensembles, providing a robust and model-aware approach to dimensionality reduction. In parallel, an external tool-based approach using the Featurewiz library was evaluated, implementing a

Minimum Redundancy Maximum Relevance (MRMR) criterion [108]. MRMR selects features that are highly relevant to the target variable while minimizing redundancy across the feature set, ensuring a compact yet informative representation. Across multiple experiments, MRMR consistently outperformed alternative strategies and was therefore adopted for all subsequent analyses, reducing the feature set to 50 features per epoch, which balanced model complexity with predictive performance.

2.4. Classification Models and Evaluation Protocol

2.4.1. Baseline Models and Conditional Hyperparameter Optimization

To identify optimal features and classifiers, we initially evaluated the following models: Support Vector Machine (SVM), K Nearest Neighbors (KNN), Gradient Boosting, Extra Trees, Random Forest, Decision Trees, Logistic Regression, AdaBoost, Naive Bayes, and a Multilayer Perceptron (MLP). Hyperparameters were not tuned initially, and evaluation was conducted using various sets of feature arrays. A 50-50 random training-testing split was used to evaluate the accuracy of every model on the features array.

2.4.2. Ensemble Learning via Voting and Stacking

Voting and Stacking Ensemble methods have a rich history of usage in machine learning [81], as they enable the aggregation of predictions from multiple models to leverage their individual strengths while mitigating their weaknesses. In this study, Support Vector Machines (SVM), k-Nearest Neighbors (KNN), Gradient Boosting, and Extremely Randomized Trees were employed as base learners within both voting and stacking ensemble frameworks. These ensemble approaches integrate predictions from the individual models using different strategies to improve overall predictive performance. Specifically, the voting classifier combines model outputs either through a hard majority voting scheme or through a soft voting mechanism that averages the predicted class probabilities across all classifiers. In addition, a stacking approach was implemented, in which a logistic regression meta-classifier learns to capture more complex patterns in the data by using the predictions of the base models as input features.

2.4.3. Feature Bagging and Data Resampling Ensembles

To improve robustness to feature selection variability and sample heterogeneity, two additional ensemble strategies were implemented.

(a) Diverse Feature Bagging

Random subsets of features were generated from the selected feature pool (Figure 2). For each subset, classifiers were trained independently and evaluated on a validation set. Only models achieving validation accuracy above a predefined threshold were retained. Predictions from the retained models were combined using soft voting. For low-confidence predictions (posterior probability < 0.9), a secondary ensemble decision was applied to refine the final classification.

(b) Segmented Data Bagging

In the segmented data bagging approach, the training dataset was partitioned into multiple segments treated as independent training sets. Bootstrap resampling was applied within each segment, and multiple classifiers were trained on these resampled subsets. Final predictions were obtained by aggregating segment-level predictions using majority voting and meta-classification.

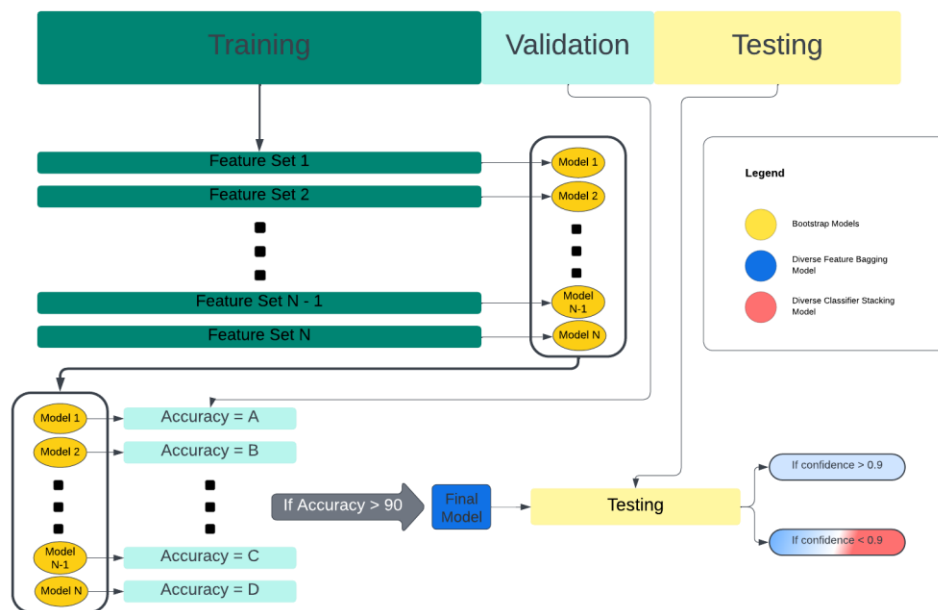


Figure 2. Diverse Feature Bagging Classifier.

2.4.4. Evaluation Protocol

Data were split into training and testing sets using a 50/50 split. Model performance was evaluated using accuracy, precision, recall, F1-score, and confusion matrices [109]. For ensemble models, both predictive accuracy and confidence calibration were examined [110]. Final performance metrics were reported on held-out test data only.

Classification was performed using multiple machine learning models, including Support Vector Machines (SVM), k-Nearest Neighbors (KNN), Gradient Boosting, Random Forests, and Extremely Randomized Trees. For SVM, a radial basis function (RBF) kernel was used:

$$K(x_i, x_j) = \exp(-\gamma \|x_i - x_j\|^2) \quad (9)$$

where x_i and x_j represent the feature vectors of the i -th and j -th samples, respectively, $\|\cdot\|$ denotes the Euclidean distance between the two feature vectors, and γ is a kernel parameter that controls the width of the Gaussian function, determining how far the influence of a single training example reaches. The RBF kernel measures the similarity between two samples: the closer x_i and x_j are in feature space, the higher the kernel value, with a maximum of 1 when they are identical.

Ensemble strategies were further explored, including hard voting, soft voting, and stacked generalization [111]. In the stacking framework, logistic regression was used as a meta-classifier, modeling the posterior probability as

$$P(y = 1|x; \theta) = \sigma(\theta^T x) = \frac{1}{1 + e^{-\theta^T x}} \quad (10)$$

where x represents the feature vector of a sample, y is the class label for the sample (with $y = 1$ indicating the positive class), θ is the vector of model parameters (weights) learned during training, $\theta^T x$ denotes the dot product between the weights and the feature vector, and $\sigma(\cdot)$ is the sigmoid function, which maps the input to a probability between 0 and 1. This equation models the posterior probability that a given sample belongs to the positive class, based on its features and the learned model parameters.

Data were split into training and testing sets using a 50/50 split. Within the training set, five-fold cross-validation was used for hyperparameter tuning, and all model performance metrics were evaluated on held-out test data, including accuracy, precision, recall, F1-score, and ROC-AUC for

binary classification [109]. These procedures ensured robust evaluation and fair comparison across models while mitigating the risk of overfitting.

3. Results

3.1. Performance on Dataset 1 (Primary Dataset)

The proposed ensemble-based classification framework achieved strong performance on Dataset 1 (see Table 2 for detailed metrics), with a test accuracy of 98.06%. Both macro-averaged and weighted F1-scores were approximately 0.98, indicating balanced performance across classes. Out of 7,206 test epochs, only 140 were misclassified, reflecting robust prediction at the epoch level.

Class-wise evaluation further highlights the model's reliability. For the healthy control group, recall was 99.24% and precision 96.60%, indicating that nearly all true control epochs were correctly identified, with a small proportion of false positives. The SZ group achieved a recall of 97.06% and precision of 99.35%, demonstrating accurate detection with relatively few false negatives. These results suggest the model effectively distinguishes between SZ and control epochs, although the use of epoch-level evaluation means some caution is warranted in extrapolating performance to independent subjects.

Table 2. Performance Metrics of Dataset 1.

Class	Precision	Recall	F1-score	Support
Control	0.966	0.9924	0.979	3292
SZ	0.9935	0.9706	0.9819	3914
Macro Avg	0.9797	0.9815	0.9805	7206
Weighted Avg	0.9809	0.9806	0.9806	7206

Comparative analysis across classifiers showed that ensemble and tree-based models performed best on this dataset (see Table 3). Extremely Randomized Trees achieved the highest single-model accuracy (98.75%), closely followed by Random Forests (98.68%). The ensemble voting classifier delivered comparably strong performance (98.06%), supporting the benefit of combining complementary classifiers. In contrast, Naive Bayes performed substantially worse (65.09% accuracy), suggesting that its strong distributional assumptions are poorly matched to the underlying EEG feature space. Overall, these findings indicate that ensemble and tree-based approaches provide near-optimal performance on Dataset 1.

Table 3. Performance of Different Classification Methods on Dataset 1.

Classification Method	Accuracy (%)	Notes
Support Vector Machine (SVM)	94.52	RBF kernel, tuned via 4-fold CV
K-Nearest Neighbors (KNN)	87.37	Tuned neighbors & weighting
Extremely Randomized Trees	98.75	Best single model
Random Forest	98.68	Tuned depth & estimators
Decision Tree	95.21	Single-tree baseline
AdaBoost	95.56	SAMME.R (deprecated warning noted)
Naive Bayes	65.09	Poor fit to feature distribution
ML Ensemble (Voting)	98.06	Best overall (test set)

We used the Receiver Operating Characteristic (ROC) curve, a standard method for evaluating the diagnostic performance of a binary classifier by illustrating the trade-off between the True Positive Rate (sensitivity) and the False Positive Rate (1 – specificity) across varying decision thresholds. Figure 3a presents the ROC curve for the proposed model on Dataset 1, showing an Area Under the Curve (AUC) of 0.998—indicative of near-perfect discrimination between schizophrenia and healthy control groups. The curve's sharp rise toward the top-left corner highlights high

sensitivity achieved at very low false positive rates. Figure 3b complements this by plotting precision, recall, and F1-score as functions of the classification threshold, revealing an optimal threshold of 0.434 where the model balances these metrics to maximize the F1-score. Such threshold tuning is critical in clinical settings, enabling customization of the decision boundary to appropriately manage the trade-off between false positives and false negatives. Together, these figures demonstrate both the model's strong predictive capability and its adaptability to optimize classification performance through threshold adjustment.

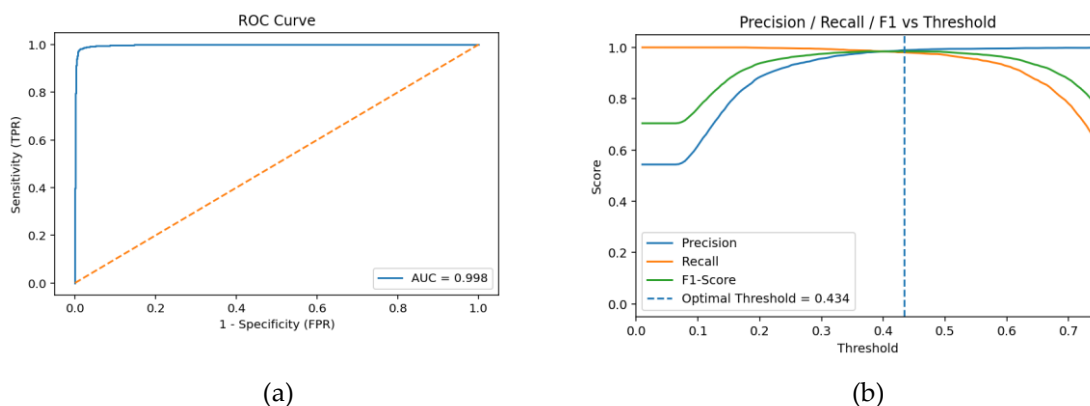


Figure 3. (a) ROC curve for Dataset 1 showing the trade-off between sensitivity (True Positive Rate) and 1-specificity (False Positive Rate) for the classifier. The curve demonstrates excellent performance with an Area Under the Curve (AUC) of 0.998, indicating high discriminative ability. (b) Precision, Recall, and F1-Score plotted against different classification thresholds for Dataset 1. The plot identifies the optimal threshold at 0.434, where the F1-Score is maximized, balancing precision and recall effectively.

These findings indicate that tree-based and ensemble frameworks are well-suited to EEG-based SZ classification, providing robust and balanced performance at the epoch level. However, generalization to new subjects and independent datasets should be interpreted cautiously, motivating further validation across external cohorts.

3.2. Performance on Dataset 2 (Independent Validation Dataset)

When evaluated on Dataset 2, the proposed framework maintained strong performance (see Table 4 for performance metrics), achieving a test accuracy of 91.47%. Macro-averaged and weighted F1-scores were both approximately 0.91, indicating balanced classification across classes despite the smaller sample size and increased dataset heterogeneity. Compared to Dataset 1, the modest reduction in performance reflects the greater difficulty of this dataset rather than model instability.

At the class level, the model demonstrated a well-balanced trade-off between sensitivity and specificity. The healthy group achieved a precision of 92.02% and a recall of 88.29%, while the SZ group showed a higher recall (93.97%) and a precision of 91.07%. The confusion matrix revealed 43 mis-classifications out of 504 samples, with errors distributed relatively symmetrically across classes.

Table 4. Performance Metrics of Dataset 2.

Class	Precision	Recall	F1-score	Support
Control	0.9202	0.8829	0.9011	222
SZ	0.9107	0.9397	0.925	282
Macro Avg	0.9154	0.9113	0.9131	504
Weighted Avg	0.9149	0.9147	0.9145	504

Consistent with the results on Dataset 1, ensemble learning delivered the strongest overall performance on Dataset 2 (see Table 5). The ensemble voting classifier achieved the highest accuracy at 91.47%, outperforming all individual models. Among single classifiers, Extremely Randomized

Trees performed best with 88.12% accuracy, followed by Random Forests at 85.89%. Baseline implementations of SVM, k-Nearest Neighbors (kNN), Naive Bayes, Decision Trees, and AdaBoost showed substantially lower accuracies, ranging from approximately 71% to 79%, underscoring the critical role of feature selection and ensemble strategies in achieving robust EEG-based schizophrenia classification.

Importantly, all preprocessing, feature extraction, and model parameters were transferred directly from Dataset 1 without additional tuning, reflecting a conservative and realistic evaluation of the framework's cross-dataset generalization. This demonstrates the model's robustness to dataset variability and highlights the advantage of ensemble approaches in improving stability and accuracy across diverse EEG data sources.

Table 5. Performance of Different Classification Methods on Dataset 2.

Classification Method	Accuracy (%)	Notes
Support Vector Machine (SVM)	71.04	Baseline only (below tuning threshold)
K-Nearest Neighbors (KNN)	75.5	Baseline only (below tuning threshold)
Extremely Randomized Trees	88.12	Tuned via 4-fold CV
Random Forest	85.89	Tuned via 4-fold CV
Decision Tree	77.23	Baseline only
AdaBoost	79.46	Baseline only
Naive Bayes	71.29	Baseline only
ML Ensemble (Voting)	91.47	Best overall (test set)

To assess the model's generalizability, we applied the Receiver Operating Characteristic (ROC) curve analysis to the independent validation Dataset 2. Figure 4a shows the ROC curve for this dataset, with an Area Under the Curve (AUC) of 0.962, indicating excellent discrimination between schizophrenia and healthy control groups despite the increased heterogeneity and smaller sample size relative to Dataset 1. The curve demonstrates consistently high sensitivity while maintaining low false positive rates across thresholds. Figure 4b further characterizes model performance by plotting precision, recall, and F1-score as functions of the classification threshold, identifying an optimal threshold of 0.502 where the model achieves a balanced trade-off and maximal F1-score of approximately 0.82. At this threshold, precision reaches about 0.85 and recall approximately 0.79, reflecting an effective balance between minimizing false positives and capturing true positives. These results confirm that the model generalizes robustly to independent data, maintaining strong predictive accuracy and offering a validated threshold for clinical application that balances detection sensitivity and specificity.

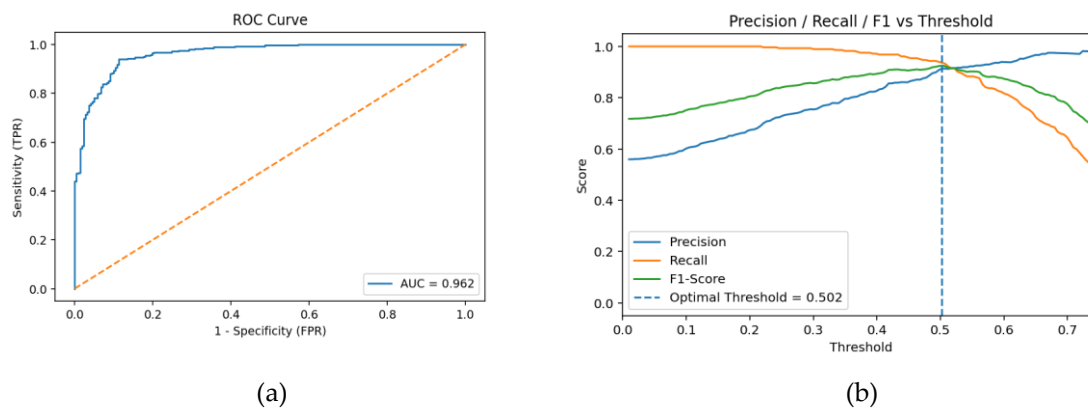


Figure 4. (a) Receiver Operating Characteristic (ROC) curve for the proposed classification model evaluated on Dataset 2. (b) Precision, recall, and F1-score plotted against classification thresholds for the proposed model on Dataset 2.

4. Discussion

This study presents a computationally efficient and interpretable EEG classification framework for schizophrenia that integrates tunable artifact suppression, multidomain feature intelligence, and advanced ensemble learning. Evaluated under a stringent cross-dataset protocol, our proposed approach achieved strong and stable performance on two independent datasets, reaching 98.06% accuracy on the primary dataset and 91.47% accuracy on an unseen validation cohort. These results approach the performance levels reported by deep learning models while offering substantially improved transparency, data efficiency, and deployability, which are key requirements for clinical neurocomputing applications.

4.1. Algorithmic Contributions: Tunable Preprocessing, Feature Intelligence, and Ensemble Design

A key novelty of this work lies in the algorithmic integration of controllable signal conditioning, optimized feature-space learning, and ensemble intelligence, rather than reliance on end-to-end deep architectures. Unlike conventional pipelines that depend solely on fixed preprocessing such as ICA, the proposed framework incorporates Automatic and Tunable Artifact Removal (ATAR), introducing an explicit control parameter (β) that enables adaptive suppression of ocular and muscle artifacts while preserving diagnostically relevant neural signals. This tunable preprocessing mechanism represents a form of computational intelligence at the signal-conditioning level, allowing robustness to be explicitly controlled rather than implicitly learned. Our results indicate that ATAR improves signal quality and downstream classification performance, particularly in datasets with substantial inter-subject variability, distinguishing this approach from standard ICA-based pipelines commonly used in prior studies [59,61,85].

Beyond preprocessing, the framework advances multi-domain feature intelligence by integrating complementary views of EEG dynamics across time, frequency, and complexity domains. In contrast to prior studies that focus on narrow feature subsets such as spectral power or band ratios [60,66–68], our model integrates time-domain statistics (mean, variance, kurtosis), frequency-domain features (power spectral density, band ratios), and entropy-based measures (sample entropy, permutation entropy). This multidimensional representation includes higher-order statistics and multiple entropy measures, capturing non-Gaussian, nonlinear, and non-stationary properties of neural signals. This richer representation enables the model to exploit subtle alterations in oscillatory structure and neural complexity known to characterize schizophrenia.

To manage the resulting high-dimensional feature space, we conducted a systematic evaluation of feature selection strategies, demonstrating that the Minimum Redundancy–Maximum Relevance (MRMR) criterion is particularly effective in retaining discriminative information while minimizing redundancy. This feature-space optimization is critical for stabilizing decision boundaries in small-to-moderate EEG datasets and constitutes an important methodological contribution beyond ad hoc feature pruning.

At the decision level, the framework extends ensemble learning beyond standard majority voting. Feature bagging, segmented data bagging, and confidence-aware prediction mechanisms were employed to improve robustness to feature variability, subject heterogeneity, and low-certainty predictions. These ensemble strategies explicitly address variance and reliability—two central challenges in EEG-based learning—and remain underexplored in schizophrenia EEG studies ([59,81]). From a neurocomputing perspective, this system-level ensemble design enhances generalization while maintaining interpretability and computational efficiency.

4.2. Stable Classification Under Data and Resource Constraints

A defining advantage of the proposed framework is its data efficiency. EEG datasets for schizophrenia are typically small, heterogeneous, and noisy, conditions under which deep learning models are prone to overfitting and unstable generalization. By combining noise-resilient preprocessing, discriminative feature selection, and ensemble learning, the proposed approach

achieves high accuracy even under limited sample sizes. The strong cross-dataset performance observed here demonstrates that carefully engineered feature-based models can generalize reliably without requiring large-scale labeled data.

From a computational standpoint, the framework offers a favorable performance–cost trade-off. Unlike deep learning approaches that require GPUs, extensive training time, and high energy consumption [66,67], the pipeline in our approach shifts computational effort to one-time preprocessing and evidence-based feature extraction. Downstream classifiers operate efficiently on standard CPU hardware, enabling training and inference in minutes rather than hours. This efficiency supports real-time or near-real-time deployment and facilitates integration into existing hospital and clinical workflows, including resource-constrained environments.

Importantly, the ensemble framework contributed substantially to performance stability across datasets. While individual classifiers (e.g., Random Forest, Extremely Randomized Trees) performed well on both Dataset 1 and Dataset 2, the soft-voting ensemble consistently outperformed single models, reducing variance and mitigating overfitting—a strategy not systematically explored in prior schizophrenia EEG studies [59,61,85]. This robustness is particularly valuable for clinical neurocomputing applications, where EEG quality and acquisition conditions vary widely.

4.3. Interpretability, Reliability, and Translational Neurocomputing Impact

Interpretability is a critical requirement for clinical decision-support systems and a key limitation of deep learning-based EEG analysis. While CNNs and RNNs can achieve high accuracy [66,67], their latent representations are difficult to map to neurophysiological mechanisms, limiting clinician trust and translational potential. In contrast, our framework maintains transparency across all processing stages, from artifact suppression to feature extraction and ensemble decision-making.

By relying on physiologically meaningful features such as spectral power, entropy, and fractal dynamics, the framework enables direct interpretation of classification outcomes in terms of known neural biomarkers. Feature importance analysis revealed consistent contributions from band-power alterations over central regions and elevated entropy measures, aligning with established findings of disrupted oscillatory activity, altered sensorimotor processing, and reduced neural complexity in schizophrenia [59,61,85]. This convergence between computational outcomes and neurophysiological theory enhances both scientific validity and clinical trust.

The confidence-aware ensemble mechanism further improves reliability by mitigating low-certainty predictions, an important consideration for clinical deployment. Unlike opaque end-to-end models, the modular and controllable nature of the proposed framework allows practitioners to adjust preprocessing strength, feature dimensionality, and decision thresholds to accommodate variable EEG quality. Such controllability is essential for handling real-world data variability and supports regulatory and translational requirements for explainable AI systems.

Importantly, interpretable features also support biomarker discovery and clinical translation. By identifying EEG patterns consistently associated with schizophrenia, the framework can inform patient stratification, monitoring of disease progression, and targeted interventions, such as neurofeedback or neuromodulation protocols aimed at normalizing oscillatory activity in affected cortical regions. Unlike purely predictive deep learning models, our approach provides actionable insights that bridge computational performance with clinical relevance.

Our proposed framework demonstrates that high classification accuracy, cross-dataset generalization, and computational efficiency can be achieved without sacrificing interpretability. By integrating noise-resilient preprocessing, multidomain feature learning, and ensemble intelligence, the approach matches or exceeds the performance of prior machine learning and deep learning methods [59,61,66,67,85] while maintaining transparent and physiologically grounded decision mechanisms. These properties are critical for advancing EEG-based schizophrenia analysis toward practical clinical neurocomputing applications.

4.4. Limitations and Future Directions

Despite the strong performance and generalizability demonstrated by the proposed framework, several limitations should be considered. First, the primary dataset consisted of only 14 patients with schizophrenia and 14 healthy controls, which may limit statistical power and the generalizability of the results. Although the model maintained robust performance on an independent validation dataset, larger and more diverse cohorts are necessary to fully establish clinical reliability. From a neurocomputing perspective, such datasets are essential for stress-testing model stability and ensemble diversity across heterogeneous acquisition conditions. Second, the Automatic and Tunable Artifact Removal (ATAR) algorithm, while effective in enhancing signal quality, has not been systematically optimized across different EEG populations or recording protocols. Systematic sensitivity analyses and standardized parameter selection strategies will be important to improve reproducibility and facilitate broader adoption. The tunable nature of ATAR, however, offers a clear pathway toward adaptive signal conditioning tailored to variable EEG quality, an advantage over fixed, one-size-fits-all preprocessing pipelines. Third, ensemble classifiers improved accuracy over single classifiers but introduce greater computational overhead, which may limit real-time or resource-constrained clinical applications. While the overall framework remains substantially more efficient than deep learning models, future work should investigate lightweight ensemble designs, model pruning, or dynamic ensemble selection to further reduce inference time and support real-time or near-real-time deployment in constrained clinical environments.

Beyond these framework-specific considerations, EEG-based schizophrenia classification continues to face systemic challenges. Public datasets remain limited in size and heterogeneous in electrode layouts, recording protocols, and participant characteristics, complicating cross-study comparison and algorithm benchmarking [59,61,66,85]. Additionally, symptom heterogeneity and class imbalance remain major obstacles to developing universally applicable classifiers.

Future research should explore multimodal neurocomputing frameworks that integrate EEG with behavioral and cognitive performance measures (e.g., [4,5]). Hybrid learning strategies, including graph-based models, attention mechanisms, or transformer-based architectures, could exploit complementary information across modalities while preserving interpretability through structured feature representations [112,113]. Such approaches could improve diagnostic precision, enable symptom profiling, and support individualized monitoring and intervention, particularly in disorders where neural dysfunction and observable behavior are tightly coupled. Key challenges will include temporal alignment, heterogeneous feature fusion, and explainability; however, ongoing advances in sensor fusion and explainable artificial intelligence offer promising directions [114].

Furthermore, progress toward clinical translation will require coordinated efforts in open data sharing, standardized preprocessing, rigorous external validation, and systematic evaluation of ensemble and hybrid learning strategies. By prioritizing controllability, interpretability, and data efficiency, future neurocomputing systems can move beyond proof-of-concept classification toward reliable, clinically actionable decision-support tools that complement traditional behavioral assessment in schizophrenia.

5. Conclusions

This study demonstrates that accurate and generalizable schizophrenia classification can be achieved from resting-state EEG using a computationally efficient and interpretable framework that integrates robust preprocessing, multidomain feature extraction, and ensemble machine learning. The proposed approach attains high accuracy on both primary and independent validation datasets, highlighting strong discriminative capability and cross-dataset robustness. By emphasizing controllable artifact removal, explicit feature representations, and ensemble intelligence rather than deep architectures, the framework delivers competitive performance with substantially lower computational cost and improved transparency. Accordingly, this method should be viewed as a complementary and practical alternative to deep learning-based neural network approaches, particularly suited for data-limited, resource-constrained, and clinically interpretable neurocomputing applications.

Author Contributions: Conceptualization, Y.Z.; methodology, Y.E., X.H., and Y.Z.; software, Y.E., Y.Z.; validation, X.H., A.Z., and Y.L.; formal analysis, Y.E., X.H.; investigation, Y.E, X.H.; resources, Y.Z.; data curation, Y.Z.; writing—original draft preparation, Y.E., X.H., Y.Z.; writing—review and editing, X.H., A.Z., Y.L., Y.Z.; visualization, Y.E, X.H.; supervision, Y.Z.; project administration, Y.Z.; funding acquisition, Y.Z.. All authors have read and agreed to the published version of the manuscript.

Funding: This research was funded by University of Minnesota’s Grant-in-Aid (GIA) of Research, Artistry, and Scholarship program and Brain Imaging Grant. Y.L. was additionally supported by the youth program of National Social Science Foundation of China (23CYY051).

Data Availability Statement: The code used for EEG preprocessing, feature extraction, and machine learning analyses in this study is publicly available on GitHub at https://github.com/yossefemara7/eeg_ml_pipeline. The two EEG datasets analyzed in this study are publicly available from their original sources and are cited in the manuscript.

Acknowledgments: The authors acknowledge the Minnesota Supercomputing Institute (MSI) at the University of Minnesota for providing resources that contributed to the research results reported within this paper. During the preparation of this manuscript/study, the authors used ChatGPT (version GPT-4o) for improving grammar and text clarity. The authors have reviewed and edited the output and take full responsibility for the content of this publication.

Conflicts of Interest: The authors declare no conflicts of interest.

Abbreviations

The following abbreviations are used in this manuscript:

ADHD	Attention-Deficit/Hyperactivity Disorder
AdaBoost	Adaptive Boosting
ANN	Artificial Neural Network
ATAR	Automatic and Tunable Artifact Removal
AUC	Area Under the Curve
BH	Black Hole (optimization algorithm)
BSS	Blind Source Separation
BT	Boosted Tree
CGP17Pat	Cartesian Genetic Programming 17 Pattern
CNN	Convolutional Neural Network
CV	Cross-Validation
DFA	Detrended Fluctuation Analysis
DL	Deep Learning
DT	Decision Tree
EDF	European Data Format
EEG	Electroencephalography
ERP	Event-Related Potential
FFT	Fast Fourier Transform
FIR	Finite Impulse Response
F-LSSVM	Flexible Least Squares Support Vector Machine
F-TQWT	Flexible Tunable Q Wavelet Transform
GWO	Grey Wolf Optimization
HA	Hjorth Activity
HC	Hjorth Complexity
HM	Hjorth Mobility
ICA	Independent Component Analysis
ICD-10	International Classification of Diseases, 10th Revision
INCA	Iterative Neighborhood Component Analysis
IPN	Institute of Psychiatry and Neurology
KNN	k-Nearest Neighbors
LDA	Linear Discriminant Analysis
LNNCI	Laboratory for Neurophysiology and Neuro-Computer Interfaces

LOO	Leave-One-Out
LOSO	Leave-One-Subject-Out
LSTM	Long Short-Term Memory
MI	Mutual Information
ML	Machine Learning
MLP	Multilayer Perceptron
MHRC	Mental Health Research Center
MNE	Minimum Norm Estimation (Python library)
MRMR	Minimum Redundancy Maximum Relevance
NB	Naive Bayes
PLV	Phase-Locking Value
PNN	Probabilistic Neural Network
PSD	Power Spectral Density
RBF	Radial Basis Function
RF	Random Forest
RFE	Recursive Feature Elimination
RMS	Root Mean Square
RNN	Recurrent Neural Network
ROC	Receiver Operating Characteristic
RVMD	Robust Variational Mode Decomposition
SAMME.R	Stagewise Additive Modeling using a Multiclass Exponential Loss Function
SLBP	Symmetrically Weighted Local Binary Patterns
SpKit	Signal Processing Toolkit
SVM	Support Vector Machine
SZ (SCZ)	Schizophrenia
θ	Theta Frequency Band
α	Alpha Frequency Band
β	Beta Frequency Band
δ	Delta Frequency Band

References

1. Van Os, J.; Kapur, S. Schizophrenia. *The Lancet* **2009**, *374*, 635–645, doi:10.1016/S0140-6736(09)60995-8.
2. Teixeira, F.L.; Costa, M.R.E.; Abreu, J.P.; Cabral, M.; Soares, S.P.; Teixeira, J.P. A Narrative Review of Speech and EEG Features for Schizophrenia Detection: Progress and Challenges. *Bioeng. Basel Switz.* **2023**, *10*, doi:10.3390/bioengineering10040493.
3. Mangelinckx, C.; Belge, J.B.; Maurage, P.; Constant, E. Impaired Facial and Vocal Emotion Decoding in Schizophrenia Is Underpinned by Basic Perceptivo-Motor Deficits. *Cognit. Neuropsychiatry* **2017**, *22*, 461–467, doi:10.1080/13546805.2017.1382342.
4. Lin, Y.; Li, C.; Hu, R.; Zhou, L.; Ding, H.; Fan, Q.; Zhang, Y. Impaired Emotion Perception in Schizophrenia Shows Sex Differences with Channel- and Category-Specific Effects: A Pilot Study. *J. Psychiatr. Res.* **2023**, *161*, 150–157, doi:10.1016/j.jpsychires.2023.03.011.
5. Lin, Y.; Li, C.; Wang, X.; Song, Y.; Ding, H.; Fan, Q.; Zhang, Y. Channel- and Category-Specific Emotion Recognition Deficits and Their Associations with Symptomatology and Cognition in Individuals with Schizophrenia. *Schizophr. Res.* **2023**, *254*, 37–39, doi:10.1016/j.schres.2023.02.010.
6. Ding, H.; Zhang, Y. Speech Prosody in Mental Disorders. *Annu. Rev. Linguist.* **2023**, *9*, 335–355, doi:10.1146/annurev-linguistics-030421-065139.
7. Lin, Y.; Ding, H.; Zhang, Y. Emotional Prosody Processing in Schizophrenic Patients: A Selective Review and Meta-Analysis. *J. Clin. Med.* **2018**, *7*, 363, doi:10.3390/jcm7100363.
8. Murashko, A.A.; Shmukler, A. EEG Correlates of Face Recognition in Patients with Schizophrenia Spectrum Disorders: A Systematic Review. *Clin. Neurophysiol.* **2019**, *130*, 986–996, doi:10.1016/j.clinph.2019.03.027.
9. Boutros, N.N.; Arfken, C.; Galderisi, S.; Warrick, J.; Pratt, G.; Iacono, W. The Status of Spectral EEG Abnormality as a Diagnostic Test for Schizophrenia. *Schizophr. Res.* **2008**, *99*, 225–237, doi:10.1016/j.schres.2007.11.020.

10. Domingos, C.; Więclawski, W.; Frycz, S.; Wojcik, M.; Jáni, M.; Dudzińska, O.; Adamczyk, P.; Ros, T. Functional Connectivity in Chronic Schizophrenia: An EEG Resting-State Study with Corrected Imaginary Phase-Locking. *Brain Behav.* **2025**, *15*, e70370, doi:10.1002/brb3.70370.
11. Chen, H.; Lei, Y.; Li, R.; Xia, X.; Cui, N.; Chen, X.; Liu, J.; Tang, H.; Zhou, J.; Huang, Y.; et al. Resting-State EEG Dynamic Functional Connectivity Distinguishes Non-Psychotic Major Depression, Psychotic Major Depression and Schizophrenia. *Mol. Psychiatry* **2024**, doi:10.1038/s41380-023-02395-3.
12. van der Stelt, O.; Belger, A. Application of Electroencephalography to the Study of Cognitive and Brain Functions in Schizophrenia. *Schizophr. Bull.* **2007**, *33*, 955–970, doi:10.1093/schbul/sbm016.
13. Sengoku, A.; Takagi, S. Electroencephalographic Findings in Functional Psychoses: State or Trait Indicators? *Psychiatry Clin. Neurosci.* **1998**, *52*, 375–381, doi:10.1046/j.1440-1819.1998.00414.x.
14. Rahul, J.; Sharma, D.; Sharma, L.D.; Nanda, U.; Sarkar, A.K. A Systematic Review of EEG Based Automated Schizophrenia Classification through Machine Learning and Deep Learning. *Front. Hum. Neurosci.* **2024**, *18*, 1347082, doi:10.3389/fnhum.2024.1347082.
15. Ravan, M.; Noroozi, A.; Sanchez, M.M.; Borden, L.; Alam, N.; Flor-Henry, P.; Colic, S.; Khodayari-Rostamabad, A.; Minuzzi, L.; Hasey, G. Diagnostic Deep Learning Algorithms That Use Resting EEG to Distinguish Major Depressive Disorder, Bipolar Disorder, and Schizophrenia from Each Other and from Healthy Volunteers. *J. Affect. Disord.* **2024**, *346*, 285–298, doi:10.1016/j.jad.2023.11.017.
16. Guo, Z.; Wang, J.; Jing, T.; Fu, L. Investigating the Interpretability of Schizophrenia EEG Mechanism through a 3DCNN-Based Hidden Layer Features Aggregation Framework. *Comput. Methods Programs Biomed.* **2024**, *247*, 108105, doi:10.1016/j.cmpb.2024.108105.
17. Parsa, M.; Rad, H.Y.; Vaezi, H.; Hossein-Zadeh, G.-A.; Setarehdan, S.K.; Rostami, R.; Rostami, H.; Vahabie, A.-H. EEG-Based Classification of Individuals with Neuropsychiatric Disorders Using Deep Neural Networks: A Systematic Review of Current Status and Future Directions. *Comput. Methods Programs Biomed.* **2023**, *240*, 107683, doi:10.1016/j.cmpb.2023.107683.
18. Kose, M.R.; Ahirwal, M.K.; Atulkar, M. Weighted Ordinal Connection Based Functional Network Classification for Schizophrenia Disease Detection Using EEG Signal. *Phys. Eng. Sci. Med.* **2023**, *46*, 1055–1070, doi:10.1007/s13246-023-01273-0.
19. Lin, P.; Zhu, G.; Xu, X.; Wang, Z.; Li, X.; Li, B. Brain Network Analysis of Working Memory in Schizophrenia Based on Multi Graph Attention Network. *Brain Res.* **2024**, *1831*, 148816, doi:10.1016/j.brainres.2024.148816.
20. Li, F.; Wang, G.; Jiang, L.; Yao, D.; Xu, P.; Ma, X.; Dong, D.; He, B. Disease-Specific Resting-State EEG Network Variations in Schizophrenia Revealed by the Contrastive Machine Learning. *Brain Res. Bull.* **2023**, *202*, 110744, doi:10.1016/j.brainresbull.2023.110744.
21. Baygin, M.; Barua, P.D.; Chakraborty, S.; Tuncer, I.; Dogan, S.; Palmer, E.; Tuncer, T.; Kamath, A.P.; Ciaccio, E.J.; Acharya, U.R. CCPNet136: Automated Detection of Schizophrenia Using Carbon Chain Pattern and Iterative TQWT Technique with EEG Signals. *Physiol. Meas.* **2023**, *44*, doi:10.1088/1361-6579/acb03c.
22. Diykh, M.; Li, Y.; Wen, P. EEG Sleep Stages Classification Based on Time Domain Features and Structural Graph Similarity. *IEEE Trans. Neural Syst. Rehabil. Eng.* **2016**, *24*, 1159–1168, doi:10.1109/TNSRE.2016.2552539.
23. Wang, B.; Otten, L.J.; Schulze, K.; Afrah, H.; Varney, L.; Cotic, M.; Saadullah Khani, N.; Linden, J.F.; Kuchenbaecker, K.; McQuillin, A.; et al. Is Auditory Processing Measured by the N100 an Endophenotype for Psychosis? A Family Study and a Meta-Analysis. *Psychol. Med.* **2024**, *54*, 1559–1572, doi:10.1017/S0033291723003409.
24. Hamilton, H.K.; Mathalon, D.H.; Ford, J.M. P300 in Schizophrenia: Then and Now. *Biol. Psychol.* **2024**, *187*, 108757, doi:10.1016/j.biopsycho.2024.108757.
25. Faust, O.; Acharya, U.R.; Min, L.C.; Spath, B.H.C. AUTOMATIC IDENTIFICATION OF EPILEPTIC AND BACKGROUND EEG SIGNALS USING FREQUENCY DOMAIN PARAMETERS. *Int. J. Neural Syst.* **2010**, *20*, 159–176, doi:10.1142/S0129065710002334.
26. Jia, Y.; Jariwala, N.; Hinkley, L.B.N.; Nagarajan, S.; Subramaniam, K. Abnormal Resting-State Functional Connectivity Underlies Cognitive and Clinical Symptoms in Patients with Schizophrenia. *Front. Hum. Neurosci.* **2023**, *17*, 1077923, doi:10.3389/fnhum.2023.1077923.

27. Cao, Y.; Han, C.; Peng, X.; Su, Z.; Liu, G.; Xie, Y.; Zhang, Y.; Liu, J.; Zhang, P.; Dong, W.; et al. Correlation Between Resting Theta Power and Cognitive Performance in Patients With Schizophrenia. *Front. Hum. Neurosci.* **2022**, *16*, 853994, doi:10.3389/fnhum.2022.853994.
28. Madhavan, S.; Tripathy, R.K.; Pachori, R.B. Time-Frequency Domain Deep Convolutional Neural Network for the Classification of Focal and Non-Focal EEG Signals. *IEEE Sens. J.* **2020**, *20*, 3078–3086, doi:10.1109/JSEN.2019.2956072.
29. Khare, S.K.; Bajaj, V.; Acharya, U.R. SchizoNET: A Robust and Accurate Margenau–Hill Time-Frequency Distribution Based Deep Neural Network Model for Schizophrenia Detection Using EEG Signals. *Physiol. Meas.* **2023**, *44*, 035005, doi:10.1088/1361-6579/acbc06.
30. Xu, X.; Zhu, G.; Li, B.; Lin, P.; Li, X.; Wang, Z. Automated Diagnosis of Schizophrenia Based on Spatial–Temporal Residual Graph Convolutional Network. *Biomed. Eng. OnLine* **2024**, *23*, 55, doi:10.1186/s12938-024-01250-y.
31. Zhao, Z.; Li, J.; Niu, Y.; Wang, C.; Zhao, J.; Yuan, Q.; Ren, Q.; Xu, Y.; Yu, Y. Classification of Schizophrenia by Combination of Brain Effective and Functional Connectivity. *Front. Neurosci.* **2021**, *15*, 651439, doi:10.3389/fnins.2021.651439.
32. Olejarczyk, E.; Jernajczyk, W. Graph-Based Analysis of Brain Connectivity in Schizophrenia. *PLOS ONE* **2017**, *12*, e0188629, doi:10.1371/journal.pone.0188629.
33. Gajic, D.; Djurovic, Z.; Gligorijevic, J.; Di Gennaro, S.; Savic-Gajic, I. Detection of Epileptiform Activity in EEG Signals Based on Time-Frequency and Non-Linear Analysis. *Front. Comput. Neurosci.* **2015**, *9*, doi:10.3389/fncom.2015.00038.
34. Shoeibi, A.; Sadeghi, D.; Moridian, P.; Ghassemi, N.; Heras, J.; Alizadehsani, R.; Khadem, A.; Kong, Y.; Nahavandi, S.; Zhang, Y.-D.; et al. Automatic Diagnosis of Schizophrenia in EEG Signals Using CNN-LSTM Models. *Front. Neuroinformatics* **2021**, *15*, 777977, doi:10.3389/fninf.2021.777977.
35. Keihani, A.; Sajadi, S.S.; Hasani, M.; Ferrarelli, F. Bayesian Optimization of Machine Learning Classification of Resting-State EEG Microstates in Schizophrenia: A Proof-of-Concept Preliminary Study Based on Secondary Analysis. *Brain Sci.* **2022**, *12*, 1497, doi:10.3390/brainsci12111497.
36. Baradits, M.; Bitter, I.; Czobor, P. Multivariate Patterns of EEG Microstate Parameters and Their Role in the Discrimination of Patients with Schizophrenia from Healthy Controls. *Psychiatry Res.* **2020**, *288*, 112938, doi:10.1016/j.psychres.2020.112938.
37. Kim, K.; Duc, N.T.; Choi, M.; Lee, B. EEG Microstate Features for Schizophrenia Classification. *PloS One* **2021**, *16*, e0251842, doi:10.1371/journal.pone.0251842.
38. Thilakvathi, B.; Shenbaga, D.S.; Bhanu, K.; Malaippan, M. EEG Signal Complexity Analysis for Schizophrenia during Rest and Mental Activity. *Biomed. Res.* **2017**, *28*.
39. Jahmunah, V.; Lih Oh, S.; Rajinikanth, V.; Ciaccio, E.J.; Hao Cheong, K.; Arunkumar, N.; Acharya, U.R. Automated Detection of Schizophrenia Using Nonlinear Signal Processing Methods. *Artif. Intell. Med.* **2019**, *100*, 101698, doi:10.1016/j.artmed.2019.07.006.
40. Li, F.; Wang, J.; Liao, Y.; Yi, C.; Jiang, Y.; Si, Y.; Peng, W.; Yao, D.; Zhang, Y.; Dong, W.; et al. Differentiation of Schizophrenia by Combining the Spatial EEG Brain Network Patterns of Rest and Task P300. *IEEE Trans. Neural Syst. Rehabil. Eng.* **2019**, *27*, 594–602, doi:10.1109/TNSRE.2019.2900725.
41. Chang, Q.; Li, C.; Tian, Q.; Bo, Q.; Zhang, J.; Xiong, Y.; Wang, C. Classification of First-Episode Schizophrenia, Chronic Schizophrenia and Healthy Control Based on Brain Network of Mismatch Negativity by Graph Neural Network. *IEEE Trans. Neural Syst. Rehabil. Eng. Publ. IEEE Eng. Med. Biol. Soc.* **2021**, *29*, 1784–1794, doi:10.1109/TNSRE.2021.3105669.
42. Tikka, S.K.; Singh, B.K.; Nizamie, S.H.; Garg, S.; Mandal, S.; Thakur, K.; Singh, L.K. Artificial Intelligence-Based Classification of Schizophrenia: A High Density Electroencephalographic and Support Vector Machine Study. *Indian J. Psychiatry* **2020**, *62*, 273–282, doi:10.4103/psychiatry.IndianJPsychiatry_91_20.
43. Racz, F.S.; Stylianou, O.; Mukli, P.; Eke, A. Multifractal and Entropy-Based Analysis of Delta Band Neural Activity Reveals Altered Functional Connectivity Dynamics in Schizophrenia. *Front. Syst. Neurosci.* **2020**, *14*, 49, doi:10.3389/fnsys.2020.00049.

44. Tian, Q.; Yang, N.-B.; Fan, Y.; Dong, F.; Bo, Q.-J.; Zhou, F.-C.; Zhang, J.-C.; Li, L.; Yin, G.-Z.; Wang, C.-Y.; et al. Detection of Schizophrenia Cases From Healthy Controls With Combination of Neurocognitive and Electrophysiological Features. *Front. Psychiatry* **2022**, *13*, 810362, doi:10.3389/fpsy.2022.810362.
45. Park, S.M.; Jeong, B.; Oh, D.Y.; Choi, C.-H.; Jung, H.Y.; Lee, J.-Y.; Lee, D.; Choi, J.-S. Identification of Major Psychiatric Disorders From Resting-State Electroencephalography Using a Machine Learning Approach. *Front. Psychiatry* **2021**, *12*, 707581, doi:10.3389/fpsy.2021.707581.
46. Sharma, M.; Acharya, U.R. Automated Detection of Schizophrenia Using Optimal Wavelet-Based L1 Norm Features Extracted from Single-Channel EEG. *Cogn. Neurodyn.* **2021**, *15*, 661–674, doi:10.1007/s11571-020-09655-w.
47. Siuly, S.; Khare, S.K.; Bajaj, V.; Wang, H.; Zhang, Y. A Computerized Method for Automatic Detection of Schizophrenia Using EEG Signals. *IEEE Trans. Neural Syst. Rehabil. Eng. Publ. IEEE Eng. Med. Biol. Soc.* **2020**, *28*, 2390–2400, doi:10.1109/TNSRE.2020.3022715.
48. Prabhakar, S.K.; Rajaguru, H.; Kim, S.-H. Schizophrenia EEG Signal Classification Based on Swarm Intelligence Computing. *Comput. Intell. Neurosci.* **2020**, *2020*, 8853835, doi:10.1155/2020/8853835.
49. Aksoy, G.; Cattan, G.; Chakraborty, S.; Karabatak, M. Quantum Machine-Based Decision Support System for the Detection of Schizophrenia from EEG Records. *J. Med. Syst.* **2024**, *48*, 29, doi:10.1007/s10916-024-02048-0.
50. Oh, S.L.; Vicnesh, J.; Ciaccio, E.J.; Yuvaraj, R.; Acharya, U.R. Deep Convolutional Neural Network Model for Automated Diagnosis of Schizophrenia Using EEG Signals. *Appl. Sci.* **2019**, *9*, 2870, doi:10.3390/app9142870.
51. Korda, A.I.; Ventouras, E.; Asvestas, P.; Toumaian, M.; Matsopoulos, G.K.; Smyrnis, N. Convolutional Neural Network Propagation on Electroencephalographic Scalograms for Detection of Schizophrenia. *Clin. Neurophysiol. Off. J. Int. Fed. Clin. Neurophysiol.* **2022**, *139*, 90–105, doi:10.1016/j.clinph.2022.04.010.
52. Phang, C.-R.; Noman, F.; Hussain, H.; Ting, C.-M.; Ombao, H. A Multi-Domain Connectome Convolutional Neural Network for Identifying Schizophrenia From EEG Connectivity Patterns. *IEEE J. Biomed. Health Inform.* **2020**, *24*, 1333–1343, doi:10.1109/JBHI.2019.2941222.
53. Singh, K.; Singh, S.; Malhotra, J. Spectral Features Based Convolutional Neural Network for Accurate and Prompt Identification of Schizophrenic Patients. *Proc. Inst. Mech. Eng. [H]* **2021**, *235*, 167–184, doi:10.1177/0954411920966937.
54. Sun, J.; Cao, R.; Zhou, M.; Hussain, W.; Wang, B.; Xue, J.; Xiang, J. A Hybrid Deep Neural Network for Classification of Schizophrenia Using EEG Data. *Sci. Rep.* **2021**, *11*, 4706, doi:10.1038/s41598-021-83350-6.
55. Ahmedt-Aristizabal, D.; Fernando, T.; Denman, S.; Robinson, J.E.; Sridharan, S.; Johnston, P.J.; Laurens, K.R.; Fookes, C. Identification of Children at Risk of Schizophrenia via Deep Learning and EEG Responses. *IEEE J. Biomed. Health Inform.* **2021**, *25*, 69–76, doi:10.1109/JBHI.2020.2984238.
56. Shah, S.J.H.; Albishri, A.; Kang, S.S.; Lee, Y.; Sponheim, S.R.; Shim, M. ETSNet: A Deep Neural Network for EEG-Based Temporal-Spatial Pattern Recognition in Psychiatric Disorder and Emotional Distress Classification. *Comput. Biol. Med.* **2023**, *158*, 106857, doi:10.1016/j.combiomed.2023.106857.
57. Almadhor, A.; Ojo, S.; Nathaniel, T.I.; Alsubai, S.; Alharthi, A.; Hejaili, A.A.; Sampedro, G.A. An Interpretable XAI Deep EEG Model for Schizophrenia Diagnosis Using Feature Selection and Attention Mechanisms. *Front. Oncol.* **2025**, *15*, doi:10.3389/fonc.2025.1630291.
58. Ranjan, R.; Sahana, B.C. Multiresolution Feature Fusion for Smart Diagnosis of Schizophrenia in Adolescents Using EEG Signals. *Cogn. Neurodyn.* **2024**, *18*, 2779–2807, doi:10.1007/s11571-024-10120-1.
59. Agarwal, M.; Singhal, A. Fusion of Pattern-Based and Statistical Features for Schizophrenia Detection from EEG Signals. *Med. Eng. Phys.* **2023**, *112*, 103949, doi:10.1016/j.medengphy.2023.103949.
60. Khare, S.K.; Bajaj, V. A Hybrid Decision Support System for Automatic Detection of Schizophrenia Using EEG Signals. *Comput. Biol. Med.* **2022**, *141*, 105028, doi:10.1016/j.combiomed.2021.105028.
61. Zandbagleh, A.; Mirzakuchaki, S.; Daliri, M.R.; Premkumar, P.; Sanei, S. Classification of Low and High Schizotypy Levels via Evaluation of Brain Connectivity. *Int. J. Neural Syst.* **2022**, *32*, 2250013, doi:10.1142/S0129065722500137.

62. Azizi, S.; Hier, D.B.; Wunsch, D.C. Schizophrenia Classification Using Resting State EEG Functional Connectivity: Source Level Outperforms Sensor Level. *Annu. Int. Conf. IEEE Eng. Med. Biol. Soc. IEEE Eng. Med. Biol. Soc. Annu. Int. Conf.* **2021**, *2021*, 1770–1773, doi:10.1109/EMBC46164.2021.9630713.
63. Ciprian, C.; Masychev, K.; Ravan, M.; Manimaran, A.; Deshmukh, A. Diagnosing Schizophrenia Using Effective Connectivity of Resting-State EEG Data. *Algorithms* **2021**, *14*, 139, doi:10.3390/a14050139.
64. Shim, M.; Hwang, H.-J.; Kim, D.-W.; Lee, S.-H.; Im, C.-H. Machine-Learning-Based Diagnosis of Schizophrenia Using Combined Sensor-Level and Source-Level EEG Features. *Schizophr. Res.* **2016**, *176*, 314–319, doi:10.1016/j.schres.2016.05.007.
65. Aydemir, E.; Dogan, S.; Baygin, M.; Ooi, C.P.; Barua, P.D.; Tuncer, T.; Acharya, U.R. CGP17Pat: Automated Schizophrenia Detection Based on a Cyclic Group of Prime Order Patterns Using EEG Signals. *Healthc. Basel Switz.* **2022**, *10*, doi:10.3390/healthcare10040643.
66. Siuly, S.; Guo, Y.; Alcin, O.F.; Li, Y.; Wen, P.; Wang, H. Exploring Deep Residual Network Based Features for Automatic Schizophrenia Detection from EEG. *Phys. Eng. Sci. Med.* **2023**, *46*, 561–574, doi:10.1007/s13246-023-01225-8.
67. Siuly, S.; Li, Y.; Wen, P.; Alcin, O.F. SchizoGoogLeNet: The GoogLeNet-Based Deep Feature Extraction Design for Automatic Detection of Schizophrenia. *Comput. Intell. Neurosci.* **2022**, *2022*, 1992596, doi:10.1155/2022/1992596.
68. Supakar, R.; Satvaya, P.; Chakrabarti, P. A Deep Learning Based Model Using RNN-LSTM for the Detection of Schizophrenia from EEG Data. *Comput. Biol. Med.* **2022**, *151*, 106225, doi:10.1016/j.compbiomed.2022.106225.
69. Polat, H. Brain Functional Connectivity Based on Phase Lag Index of Electroencephalography for Automated Diagnosis of Schizophrenia Using Residual Neural Networks. *J. Appl. Clin. Med. Phys.* **2023**, *24*, e14039, doi:10.1002/acm2.14039.
70. Ferrara, M.; Franchini, G.; Funaro, M.; Cutroni, M.; Valier, B.; Toffanin, T.; Palagini, L.; Zerbinati, L.; Folesani, F.; Murri, M.B.; et al. Machine Learning and Non-Affective Psychosis: Identification, Differential Diagnosis, and Treatment. *Curr. Psychiatry Rep.* **2022**, *24*, 925–936, doi:10.1007/s11920-022-01399-0.
71. Balasubramanian, K.; Ramya, K.; Gayathri Devi, K. Optimized Adaptive Neuro-Fuzzy Inference System Based on Hybrid Grey Wolf-Bat Algorithm for Schizophrenia Recognition from EEG Signals. *Cogn. Neurodyn.* **2023**, *17*, 133–151, doi:10.1007/s11571-022-09817-y.
72. Najafzadeh, H.; Esmaeili, M.; Farhang, S.; Sarbaz, Y.; Rasta, S.H. Automatic Classification of Schizophrenia Patients Using Resting-State EEG Signals. *Phys. Eng. Sci. Med.* **2021**, *44*, 855–870, doi:10.1007/s13246-021-01038-7.
73. Yu, X.; Aziz, M.Z.; Sadiq, M.T.; Jia, K.; Fan, Z.; Xiao, G. Computerized Multidomain EEG Classification System: A New Paradigm. *IEEE J. Biomed. Health Inform.* **2022**, *26*, 3626–3637, doi:10.1109/JBHI.2022.3151570.
74. Zhu, Y.; Zhu, G.; Li, B.; Yang, Y.; Zheng, X.; Xu, Q.; Li, X. Abnormality of Functional Connections in the Resting State Brains of Schizophrenics. *Front. Hum. Neurosci.* **2022**, *16*, 799881, doi:10.3389/fnhum.2022.799881.
75. Ferreira-Santos, F.; Silveira, C.; Almeida, P.R.; Palha, A.; Barbosa, F.; Marques-Teixeira, J. The Auditory P200 Is Both Increased and Reduced in Schizophrenia? A Meta-Analytic Dissociation of the Effect for Standard and Target Stimuli in the Oddball Task. *Clin. Neurophysiol. Off. J. Int. Fed. Clin. Neurophysiol.* **2012**, *123*, 1300–1308, doi:10.1016/j.clinph.2011.11.036.
76. Jang, K.-I.; Kim, S.; Kim, S.Y.; Lee, C.; Chae, J.-H. Machine Learning-Based Electroencephalographic Phenotypes of Schizophrenia and Major Depressive Disorder. *Front. Psychiatry* **2021**, *12*, 745458, doi:10.3389/fpsy.2021.745458.
77. Barros, C.; Roach, B.; Ford, J.M.; Pinheiro, A.P.; Silva, C.A. From Sound Perception to Automatic Detection of Schizophrenia: An EEG-Based Deep Learning Approach. *Front. Psychiatry* **2021**, *12*, 813460, doi:10.3389/fpsy.2021.813460.
78. Taylor, J.A.; Larsen, K.M.; Dzafic, I.; Garrido, M.I. Predicting Subclinical Psychotic-like Experiences on a Continuum Using Machine Learning. *NeuroImage* **2021**, *241*, 118329, doi:10.1016/j.neuroimage.2021.118329.
79. Liang, S.; Chen, S.; Zhao, L.; Miao, D. Categorization of Emotional Faces in Schizophrenia Patients: An ERP Study. *Neurosci. Lett.* **2019**, *713*, 134493, doi:10.1016/j.neulet.2019.134493.

80. Olejarczyk, E.; Jernajczyk, W. EEG in Schizophrenia 2017.
81. Sagi, O.; Rokach, L. Ensemble Learning: A Survey. *WIREs Data Min. Knowl. Discov.* **2018**, *8*, e1249, doi:10.1002/widm.1249.
82. Keihani, A.; Sajadi, S.S.; Hasani, M.; Ferrarelli, F. Bayesian Optimization of Machine Learning Classification of Resting-State EEG Microstates in Schizophrenia: A Proof-of-Concept Preliminary Study Based on Secondary Analysis. *Brain Sci.* **2022**, *12*, doi:10.3390/brainsci12111497.
83. Shishkin, S.L.; Ganin, I.P.; Kaplan, A.Ya. Event-Related Potentials in a Moving Matrix Modification of the P300 Brain-Computer Interface Paradigm. *Neurosci. Lett.* **2011**, *496*, 95–99, doi:10.1016/j.neulet.2011.03.089.
84. Rajesh, K.N.V.P.S.; Sunil Kumar, T. Schizophrenia Detection in Adolescents from EEG Signals Using Symmetrically Weighted Local Binary Patterns. *Annu. Int. Conf. IEEE Eng. Med. Biol. Soc. IEEE Eng. Med. Biol. Soc. Annu. Int. Conf.* **2021**, *2021*, 963–966, doi:10.1109/EMBC46164.2021.9630232.
85. Aksöz, A.; Akyüz, D.; Bayir, F.; Yildiz, N.C.; Orhanbulucu, F.; LatiFoğlu, F. Olayla İlgili Potansiyel Sinyalleri Kullanarak Şizofreninin Analizi ve Sınıflandırılması. *Comput. Sci.* **2022**, doi:10.53070/bbd.1173093.
86. Devia, C.; Mayol-Troncoso, R.; Parrini, J.; Orellana, G.; Ruiz, A.; Maldonado, P.E.; Egana, J.I. EEG Classification During Scene Free-Viewing for Schizophrenia Detection. *IEEE Trans. Neural Syst. Rehabil. Eng. Publ. IEEE Eng. Med. Biol. Soc.* **2019**, *27*, 1193–1199, doi:10.1109/TNSRE.2019.2913799.
87. Neuhaus, A.H.; Popescu, F.C.; Bates, J.A.; Goldberg, T.E.; Malhotra, A.K. Single-Subject Classification of Schizophrenia Using Event-Related Potentials Obtained during Auditory and Visual Oddball Paradigms. *Eur. Arch. Psychiatry Clin. Neurosci.* **2013**, *263*, 241–247, doi:10.1007/s00406-012-0326-7.
88. Luján, M.Á.; Mateo Sotos, J.; Torres, A.; Santos, J.L.; Quevedo, O.; Borja, A.L. Mental Disorder Diagnosis from EEG Signals Employing Automated Learning Procedures Based on Radial Basis Functions. *J. Med. Biol. Eng.* **2022**, *42*, 853–859, doi:10.1007/s40846-022-00758-9.
89. Khare, S.K.; Bajaj, V. A Self-Learned Decomposition and Classification Model for Schizophrenia Diagnosis. *Comput. Methods Programs Biomed.* **2021**, *211*, 106450, doi:10.1016/j.cmpb.2021.106450.
90. Gramfort, A.; Luessi, M.; Larson, E.; Engemann, D.A.; Strohmeier, D.; Brodbeck, C.; Goj, R.; Jas, M.; Brooks, T.; Parkkonen, L.; et al. MEG and EEG Data Analysis with MNE-Python. *Front. Neurosci.* **2013**, *7*, doi:10.3389/fnins.2013.00267.
91. Comon, P.; Jutten, C. *Handbook of Blind Source Separation*; Academic Press: Oxford UK, 2010; ISBN 978-0-12-374726-6.
92. Delorme, A.; Makeig, S. EEGLAB: An Open Source Toolbox for Analysis of Single-Trial EEG Dynamics Including Independent Component Analysis. *J. Neurosci. Methods* **2004**, *134*, 9–21, doi:10.1016/j.jneumeth.2003.10.009.
93. Oostenveld, R.; Fries, P.; Maris, E.; Schoffelen, J.-M. FieldTrip: Open Source Software for Advanced Analysis of MEG, EEG, and Invasive Electrophysiological Data. *Comput. Intell. Neurosci.* **2011**, *2011*, 156869, doi:10.1155/2011/156869.
94. Gramfort, A.; Luessi, M.; Larson, E.; Engemann, D.A.; Strohmeier, D.; Brodbeck, C.; Goj, R.; Jas, M.; Brooks, T.; Parkkonen, L.; et al. MEG and EEG Data Analysis with MNE-Python. *Front. Neurosci.* **2013**, *7*, 267, doi:10.3389/fnins.2013.00267.
95. Tamburro, G.; Fiedler, P.; Stone, D.; Haueisen, J.; Comani, S. A New ICA-Based Fingerprint Method for the Automatic Removal of Physiological Artifacts from EEG Recordings. *PeerJ* **2018**, *6*, e4380, doi:10.7717/peerj.4380.
96. Pontifex, M.B.; Gwizdala, K.L.; Parks, A.C.; Billinger, M.; Brunner, C. Variability of ICA Decomposition May Impact EEG Signals When Used to Remove Eyeblink Artifacts. *Psychophysiology* **2017**, *54*, 386–398, doi:10.1111/psyp.12804.
97. Khosla, A.; Khandnor, P.; Chand, T. A Comparative Analysis of Signal Processing and Classification Methods for Different Applications Based on EEG Signals. *Biocybern. Biomed. Eng.* **2020**, *40*, 649–690, doi:10.1016/j.bbe.2020.02.002.
98. Singh, A.K.; Krishnan, S. Trends in EEG Signal Feature Extraction Applications. *Front. Artif. Intell.* **2023**, *5*, 1072801, doi:10.3389/frai.2022.1072801.
99. Dastgoshadeh, M.; Rabiei, Z. Detection of Epileptic Seizures through EEG Signals Using Entropy Features and Ensemble Learning. *Front. Hum. Neurosci.* **2023**, *16*, 1084061, doi:10.3389/fnhum.2022.1084061.

100. Motamedi-Fakhr, S.; Moshrefi-Torbati, M.; Hill, M.; Hill, C.M.; White, P.R. Signal Processing Techniques Applied to Human Sleep EEG Signals—A Review. *Biomed. Signal Process. Control* **2014**, *10*, 21–33, doi:10.1016/j.bspc.2013.12.003.
101. Cacciotti, A.; Pappalettera, C.; Miraglia, F.; Rossini, P.M.; Vecchio, F. EEG Entropy Insights in the Context of Physiological Aging and Alzheimer's and Parkinson's Diseases: A Comprehensive Review. *GeroScience* **2024**, *46*, 5537–5557, doi:10.1007/s11357-024-01185-1.
102. Redwan, S.M.; Uddin, M.P.; Ulhaq, A.; Sharif, M.I.; Krishnamoorthy, G. Power Spectral Density-Based Resting-State EEG Classification of First-Episode Psychosis. *Sci. Rep.* **2024**, *14*, 15154, doi:10.1038/s41598-024-66110-0.
103. García-Ponsoda, S.; García-Carrasco, J.; Teruel, M.A.; Maté, A.; Trujillo, J. Feature Engineering of EEG Applied to Mental Disorders: A Systematic Mapping Study. *Appl. Intell.* **2023**, *53*, 23203–23243, doi:10.1007/s10489-023-04702-5.
104. Pappalettera, C.; Miraglia, F.; Cotelli, M.; Rossini, P.M.; Vecchio, F. Analysis of Complexity in the EEG Activity of Parkinson's Disease Patients by Means of Approximate Entropy. *GeroScience* **2022**, *44*, 1599–1607, doi:10.1007/s11357-022-00552-0.
105. Pudjihartono, N.; Fadason, T.; Kempa-Liehr, A.W.; O'Sullivan, J.M. A Review of Feature Selection Methods for Machine Learning-Based Disease Risk Prediction. *Front. Bioinforma.* **2022**, *2*, 927312, doi:10.3389/fbinf.2022.927312.
106. Pudjihartono, N.; Fadason, T.; Kempa-Liehr, A.W.; O'Sullivan, J.M. A Review of Feature Selection Methods for Machine Learning-Based Disease Risk Prediction. *Front. Bioinforma.* **2022**, *2*, doi:10.3389/fbinf.2022.927312.
107. Bulut, O.; Tan, B.; Mazzullo, E.; Syed, A. Benchmarking Variants of Recursive Feature Elimination: Insights from Predictive Tasks in Education and Healthcare. *Information* **2025**, *16*, doi:10.3390/info16060476.
108. Hanchuan Peng; Fuhui Long; Ding, C. Feature Selection Based on Mutual Information Criteria of Max-Dependency, Max-Relevance, and Min-Redundancy. *IEEE Trans. Pattern Anal. Mach. Intell.* **2005**, *27*, 1226–1238, doi:10.1109/TPAMI.2005.159.
109. Rainio, O.; Teuvo, J.; Klén, R. Evaluation Metrics and Statistical Tests for Machine Learning. *Sci. Rep.* **2024**, *14*, 6086, doi:10.1038/s41598-024-56706-x.
110. Huang, Y.; Li, W.; Macheret, F.; Gabriel, R.A.; Ohno-Machado, L. A Tutorial on Calibration Measurements and Calibration Models for Clinical Prediction Models. *J. Am. Med. Inform. Assoc. JAMIA* **2020**, *27*, 621–633, doi:10.1093/jamia/ocz228.
111. Sherazi, S.W.A.; Bae, J.-W.; Lee, J.Y. A Soft Voting Ensemble Classifier for Early Prediction and Diagnosis of Occurrences of Major Adverse Cardiovascular Events for STEMI and NSTEMI during 2-Year Follow-up in Patients with Acute Coronary Syndrome. *PLOS ONE* **2021**, *16*, e0249338, doi:10.1371/journal.pone.0249338.
112. Manickam, N.; Ponnusamy, V.; Saravanan, A. Diagnosis of Schizophrenia Using Multimodal Data and Classification Using the EEGNet Framework. *Diagnostics* **2025**, *15*, 3081, doi:10.3390/diagnostics15233081.
113. Demrozi, F.; Farmanbar, M.; Engan, K. Multimodal AI (MMAI) for next-Generation Healthcare: Data Domains, Algorithms, Challenges, and Future Perspectives. *Curr. Opin. Biomed. Eng.* **2026**, *37*, 100632, doi:10.1016/j.cobme.2025.100632.
114. Huang, W.; Shu, N. AI-Powered Integration of Multimodal Imaging in Precision Medicine for Neuropsychiatric Disorders. *Cell Rep. Med.* **2025**, *6*, 102132, doi:10.1016/j.xcrm.2025.102132.

Disclaimer/Publisher's Note: The statements, opinions and data contained in all publications are solely those of the individual author(s) and contributor(s) and not of MDPI and/or the editor(s). MDPI and/or the editor(s) disclaim responsibility for any injury to people or property resulting from any ideas, methods, instructions or products referred to in the content.